



Published in final edited form as:

J Am Chem Soc. 2017 January 11; 139(1): 79–82. doi:10.1021/jacs.6b11525.

Direct Observation of Nanosecond Water Exchange Dynamics at a Protein Metal Site

Monika Stachura^{†,||}, Saumen Chakraborty^{‡,⊥,||}, Alexander Gottberg^{§,||}, Leela Ruckthong[‡], Vincent L. Pecoraro^{‡,*}, and Lars Hemmingsen^{†,*}

[†]Department of Chemistry, University of Copenhagen, Universitetsparken 5, 2100 København Ø, Denmark [‡]Department of Chemistry, University of Michigan, Ann Arbor, Michigan 48109-1055, United States [§]CERN, 1211 Geneva 23, Switzerland

Abstract

Nanosecond ligand exchange dynamics at metal sites within proteins is essential in catalysis, metal ion transport, and regulatory metallobiochemistry. Herein we present direct observation of the exchange dynamics of water at a Cd²⁺ binding site within two *de novo* designed metalloprotein constructs using ^{111m}Cd perturbed angular correlation (PAC) of γ -rays and ¹¹³Cd NMR spectroscopy. The residence time of the Cd²⁺-bound water molecule is tens of nanoseconds at 20 °C in both proteins. This constitutes the first direct experimental observation of the residence time of Cd²⁺ coordinated water in any system, including the simple aqua ion. A Leu to Ala amino acid substitution ~10 Å from the Cd²⁺ site affects both the equilibrium constant and the residence time of water, while, surprisingly, the metal site structure, as probed by PAC spectroscopy, remains essentially unaltered. This implies that remote mutations may affect metal site dynamics, even when structure is conserved.

Interactions of water molecules with proteins and nucleic acids play a critical role in biomolecular structure, function, and dynamics.^{1–6} In particular, significant effort has been expended toward understanding the dynamics of water molecules interacting with the surface and interior organic constituents of proteins.^{7–14} Metalloproteins constitute about one-third of all known proteins,¹⁵ and ligand exchange reactions at the metal sites involving exogenous ligands, e.g. water molecules, represent the key elementary steps in metalloenzyme catalyzed reactions, regulatory biochemical processes, and transport of metal ions across cell membranes. By approaching the issue from the viewpoint of the chemistry

*Corresponding Authors. lhe@chem.ku.dk. vlpec@umich.edu.

^{||}Present Addresses

TRIUMF, 4004 Wesbrook Mall, Vancouver BC, V6T 2A3, Canada.

[⊥]Department of Chemistry and Biochemistry, The University of Mississippi, University, MS 38677, USA.

ORCID

Saumen Chakraborty: 0000-0002-9256-2769

ASSOCIATED CONTENT

Supporting Information

The Supporting Information is available free of charge on the ACS Publications website at DOI: 10.1021/jacs.6b11525.

Materials and Methods and details of data analysis (PDF)

The authors declare no competing financial interest.

of metal ions in aqueous solution, the Eigen–Wilkins mechanism highlights the rate of water exchange in the first coordination sphere as a central property, affecting the mechanism and kinetics of formation of metal ion complexes.^{16–19} Although significant progress has been made since these groundbreaking insights, it is interesting to note that all estimates of water exchange kinetics for the divalent group 12 metal ions (Zn^{2+} , Cd^{2+} , and Hg^{2+}) rely on ligand substitution experiments; i.e. no direct experimental determination has been reported, except for an estimate of the Zn^{2+} coordinated water proton residence time of 0.1–5 ns in 2.58 molal $\text{Zn}(\text{ClO}_4)_2$ solution using incoherent quasi-elastic neutron scattering (IQENS).²⁰ Several biologically relevant metal ions are expected to display nanosecond ligand exchange dynamics,^{17,18} but spectroscopic characterization of dynamics on the nanosecond to microsecond time scale^{6,9,21–23} is not trivial. For diamagnetic metal ions, which are often critically important for Lewis Acid assisted catalysis, the paucity of experimental data is due to the fact that ligand exchange dynamics on the relevant nanosecond time scales is inaccessible by most experimental techniques, although, in an elegant NMR study by Denisov and Halle, the residence time of a Ca^{2+} -bound water molecule in Calbindin $\text{D}_{9\text{k}}$ was determined within a broad range of 5 ns–7 μs .²² Clearly then, an experimental underpinning of water dynamics at protein metal sites is essential.

De novo designed peptides provide simplified biological constructs where metal binding sites can be incorporated by careful design, and the factors controlling the structural and dynamical properties of the ligand(s) bound to the metal ion can be assessed.²⁴ The **TRI** family of peptides (general sequence $\text{Ac-G}-(\text{L}_a\text{K}_b\text{A}_c\text{L}_d\text{E}_e\text{E}_f\text{K}_g)_4\text{-G-NH}_2$) that self-assemble into parallel three-stranded α -helical coiled coils (3SCC) is among the most extensively studied systems with abundant spectroscopic, structural, and kinetic data available.^{25–30} Substitution of Leu residues with soft, metal coordinating Cys residues renders preorganized homoleptic thiol-rich metal binding sites at the interior of the coiled coils suitable for binding a variety of heavy metals including Cd^{2+} .^{25–32} Herein, we report direct determination of exchange rates of a water molecule bound to Cd^{2+} ion within the two 3SCC peptides **TRIL16C** and **TRIL16CL23A** (Figure 1).

Previous work on $\text{Cd}(\text{TRIL16C})_3^-$ showed a single ^{113}Cd NMR resonance at 625 ppm, yet the $^{111\text{m}}\text{Cd}$ PAC data indicated the presence of two coexisting Cd^{2+} complexes: a pseudotetrahedral CdS_3O (O = exogenous water) species and a trigonal planar CdS_3 species,³⁴ which was supported by quantum chemical calculations.^{35,36} From these analyses, it was concluded that the two species CdS_3O and CdS_3 are in rapid chemical exchange on the NMR time scale (ms), but in slow exchange on the PAC time scale (ns). The water exchange reaction is illustrated in Figure 2, and a temperature series of PAC data is shown in Figure 3.

The PAC spectra at $-20\text{ }^\circ\text{C}$ indicate the expected presence of two nuclear quadrupole interactions (NQIs), reflecting the coexistence of CdS_3O and CdS_3 species, and that the water exchange is taking place in the slow exchange regime with ~ 100 ns or a longer lifetime of the two species. The PAC signals for both CdS_3 and CdS_3O are resolved at $-20\text{ }^\circ\text{C}$ and, therefore, used to determine the static NQI parameters for the two species for both peptides (Table S1).

The two sets of signals reflecting CdS₃O and CdS₃ species are discernible up to 1 °C for both peptides with the onset of some extent of line broadening, indicating that the water exchange is occurring in the slow to intermediate exchange regime. At 20 °C, the two signals begin to merge into a broad signal, and at 35 °C they coalesce to a single broad signal with large line widths, indicating water exchange on the intermediate time scale. With a further increase in temperature to 50 °C one signal with a smaller line width is observed, indicating that the water exchange is approaching the fast exchange regime. Another qualitative observation, which indirectly demonstrates changes in the water residence time upon the L23A substitution, is the following: The amplitude, *A*, of signals in PAC spectroscopy directly reflects the species population, and the amplitude of the CdS₃ signal increases from the spectrum (recorded at -20 °C and at 1 °C) for the **TRIL16C** peptide to that recorded for **TRIL16CL23A**, and vice versa for the CdS₃O signal (Figure 3). That is, the equilibrium constant, *K*, for water dissociation (Figure 2) is increased upon L23A substitution. We hypothesize that removal of steric bulk by replacing the Leu23 with Ala stabilizes the CdS₃ structure in **TRIL16CL23A** as compared to **TRIL16C**. While it is possible to stabilize the CdS₃ or CdS₃O metal site structure selectively by altering the first or second coordination sphere by steric control of the hydrophobes ~5 Å from the metal binding site in other TRI peptide derivatives,^{37,38} our results here show that even the Leu23Ala substitution ~10 Å away affects the relative population of the CdS₃ or CdS₃O species. More importantly in the context of the current work, the increase of the equilibrium constant, *K*, upon the L23A substitution demonstrates that the rates (*k*₁ and *k*₋₁) must also change, in a manner so as to increase $K = k_1/k_{-1}$. The quantitative assessment of the rates based on the PAC data is addressed in the following section.

The data sets at temperatures 1 to 50 °C were analyzed using the two NQIs derived at -20 °C and simulations modeling the effect of exchange dynamics on the PAC spectra, with only the lifetimes of the CdS₃ and CdS₃O species as variables (Table 1). The details of the data analysis may be found in the Supporting Information and Tables S1–S4. The remarkable agreement of the fits with the ¹¹¹mCd PAC experimental data (Figure 3 a,b) indicates that water exchange dynamics is indeed the origin of the observed changes of the spectroscopic signal with temperature. This is the first unambiguous demonstration of exchange dynamics at a biomolecular metal site using PAC spectroscopy, the first precise determination of nanosecond metal site dynamics in a biomolecule for any diamagnetic metal ion, and the first direct observation of water exchange dynamics for any of the divalent group 12 metal ions in general,^{16–18} except for the above-mentioned IQENS experiments.²⁰

The residence time of the water molecule bound to Cd²⁺ is 30 ns for **TRIL16C** and 25 ns for **TRIL16CL23A** at 20 °C (Table 1), as derived from the PAC data. A broad range of rate constants for ligand binding to Cd²⁺ ion in solution has been observed ($10^5 - 5 \times 10^9 \text{ M}^{-1} \text{ s}^{-1}$),³⁹ possibly indicating that the rate depends on the type of ligand as well as the water exchange rate. In the protein, the water exchange clearly occurs via a dissociative mechanism, because the CdS₃ species is explicitly observed. This is contrary to the Cd²⁺ aqua ion, for which a negative volume of activation has been determined for bipyridine binding, indicating an associative exchange mechanism.⁴⁰ These observations indicate that the mechanism and kinetics of water association with and dissociation from the metal site in

proteins may be fine-tuned by using suitably designed protein scaffolds. The fine-tuning may be achieved directly by limiting the ingress and egress of water through the protein matrix, or indirectly by changing the metal site spectator ligands (in this case thiolates) or the coordination number. However, here we demonstrate that even more subtle changes in the amino acid sequence ~ 10 Å away from the metal site can also affect the water exchange rate, because the Leu23Ala substitution in **TRIL16CL23A** causes a systematic decrease of the residence time (τ_1) of the metal ion bound water molecule, compared to **TRIL16C**. The lifetime of the species without coordinating water (τ_{-1}) is less systematically affected (Table 1). These results suggest that either the CdS_3O structure is destabilized relative to the CdS_3 structure upon the L23A substitution or the transition state of the water dissociation reaction is stabilized, or a combination of both. The fact that the Leu23Ala substitution also shifts the equilibrium toward the CdS_3 structure (*vide supra*) provides further support of the destabilization of the CdS_3O structure in **TRIL16CL23A**. Thus, even remote mutations can affect the dynamics at metal sites in proteins, indicating that the first and second coordination sphere are not the only factors that affect the physical and chemical properties.

We next tested whether ^{113}Cd NMR spectroscopy support the interpretation of the PAC data in terms of changes in equilibrium population of CdS_3 and CdS_3O species as a function of temperature. Single resonances are observed for both peptides at all temperatures (Figure 4), indicating that the CdS_3O and CdS_3 species are in fast exchange on the NMR time scale.

The reference chemical shifts for pure CdS_3 and CdS_3O species are 684 ppm for **TRIL16Pen** (CdS_3) and 574 ppm for **TRIL12AL16C** (CdS_3O), respectively.⁴¹ The relative population of the two species determined by PAC spectroscopy then allows for prediction of the chemical shift for the two species in rapid exchange. At 1 °C the PAC data display a relative population of 34% (CdS_3) and 66% (CdS_3O) for **TRIL16C** and 41% (CdS_3) and 59% (CdS_3O) for **TRIL16CL23A**, respectively (Table S1). Thus, the predicted ^{113}Cd NMR resonances are 611 and 619 ppm for **TRIL16C** and **TRIL16CL23A**, respectively, in excellent agreement with the experimentally observed chemical shifts of 613 and 621 ppm (Figure 4). Therefore, the ^{113}Cd NMR data provide an independent test of the interpretation of the PAC data in terms of water exchange dynamics. A more downfield chemical shift is observed for both peptides with increasing temperature, reflecting a change in the population of the two species, shifting the equilibrium toward the CdS_3 species. The same trend is observed in the PAC spectroscopic data (Table 1), further corroborating the interpretation. That is, both the NMR and PAC data indicate an increase of the equilibrium constant, K , for the water dissociation reaction (Figure 2) with increasing temperature. This implies that dissociation of water from the metal site is an exothermic process, as expected.

$^{111\text{m}}\text{Cd}$ PAC spectroscopy is very sensitive to structural changes at the probe site.³⁶ Thus, it is noteworthy that the static NQI parameters for both the CdS_3O and the CdS_3 species are highly similar in **TRIL16C** and **TRIL16CL23A** (Table S1). Accordingly, the PAC data indicate that the metal site structure is essentially unchanged by the Leu23Ala amino acid substitution, yet both the equilibrium constant and the kinetics of water exchange are altered. This observation implies that even when structure is conserved, the thermodynamics and kinetics of processes at metal sites, and therefore potentially also the function, may change. This elucidation of remote site control of water exchange adds to the comprehensive

literature indicating the importance of dynamics for protein function.⁴² Moreover, our findings suggest a potentially very important caveat when interpreting data on site directed mutagenesis of natural metalloproteins. While the overall structure may appear unaltered, the water exchange dynamics could be perturbed even by changes several residues away from the metal center. Similarly, remote mutations have been shown to perturb the active site dynamics and catalytic properties of other proteins.^{43,44}

By using simplified, designed proteins and a spectroscopic technique of the appropriate time scale, we have demonstrated that ns ligand exchange rates can be determined directly for water binding to metals in well-defined α -helical coiled coils and that these exchange reactions may be controlled even by mutations several residues from the metal center. The methodology presented here is limited mainly by the relatively narrow selection of PAC isotopes.^{36,45}

Supplementary Material

Refer to Web version on PubMed Central for supplementary material.

Acknowledgments

L.H. thanks The Danish Council for Independent Research | Natural Sciences, and the Agency for Science, Technology and Innovation, Denmark, for the NICE grant. V.L.P. thanks the National Institutes of Health for financial support of this research (ES012236).

REFERENCES

1. Levitt M, Park H. *Structure*. 1993; 1:223–226. [PubMed: 8081736]
2. Hummer G. *Nat. Chem.* 2010; 2:906–907. [PubMed: 20966940]
3. Chandler D. *Nature*. 2005; 437:640–647. [PubMed: 16193038]
4. Qvist J, Persson E, Mattea C, Halle B. *Faraday Discuss.* 2009; 141:131–144. [PubMed: 19227355]
5. Denisov VP, Peters J, Horlein HD, Halle B. *Nat. Struct. Biol.* 1996; 3:505–509. [PubMed: 8646535]
6. Persson E, Halle B. *J. Am. Chem. Soc.* 2008; 130:1774–1787. [PubMed: 18183977]
7. Bellissent-Funel M-C, Hassanali A, Havenith M, Henchman R, Pohl P, Sterpone F, van der Spoel D, Xu Y, Garcia AE. *Chem. Rev.* 2016; 116:7673–7697. [PubMed: 27186992]
8. King JT, Arthur EJ, Brooks CL III, Kubarych KJ. *J. Am. Chem. Soc.* 2014; 136:188–194. [PubMed: 24341684]
9. Ross MR, White AM, Yu F, King JT, Pecoraro VL, Kubarych KJ. *J. Am. Chem. Soc.* 2015; 137:10164–10176. [PubMed: 26247178]
10. Huang K-Y, Kingsley CN, Sheil R, Cheng C-Y, Bierma JC, Roskamp KW, Khago D, Martin RW, Han S. *J. Am. Chem. Soc.* 2016; 138:5392–5402. [PubMed: 27052457]
11. Nucci NV, Pometun MS, Wand AJ. *Nat. Struct. Mol. Biol.* 2011; 18:245–249. [PubMed: 21196937]
12. Jia M, Yang J, Qin Y, Wang D, Pan H, Wang L, Xu J, Zhong D. *J. Phys. Chem. Lett.* 2015; 6:5100–5105. [PubMed: 26636354]
13. Wood K, Frölich A, Paciaroni A, Moulin M, Härtlein M, Zaccai G, Tobias DJ, Weik M. *J. Am. Chem. Soc.* 2008; 130:4586–4587. [PubMed: 18338890]
14. Pal SK, Peon J, Zewail AH. *Proc. Natl. Acad. Sci. U. S. A.* 2002; 99:1763–1768. [PubMed: 11842218]
15. Andreini C, Bertini I, Cavallaro G, Holliday G, Thornton J. *JBIC, J. Biol. Inorg. Chem.* 2008; 13:1205–1218. [PubMed: 18604568]
16. Richens DT. *Chem. Rev.* 2005; 105:1961–2002. [PubMed: 15941207]

17. Helm L, Merbach AE. *Chem. Rev.* 2005; 105:1923–1960. [PubMed: 15941206]
18. Helm L, Nicolle GM, Merbach AE. *Adv. Inorg. Chem.* 2005; 57:327.
19. Eigen M, Wilkins RG. *Adv. Chem. Ser.* 1965; 49:55–67.
20. Salmon P, Bellissent-Funel M-C, Herdman G. *J. Phys.: Condens. Matter.* 1990; 2:4297.
21. Hansen DF, Westler WM, Kunze MBA, Markley JL, Weinhold F, Led JJ. *J. Am. Chem. Soc.* 2012; 134:4670–4682. [PubMed: 22329704]
22. Denisov VP, Halle B. *J. Am. Chem. Soc.* 1995; 117:8456–8465.
23. Zang C, Stevens JA, Link JJ, Guo L, Wang L, Zhong D. *J. Am. Chem. Soc.* 2009; 131:2846–2852. [PubMed: 19203189]
24. Ghosh D, Pecoraro VL. *Inorg. Chem.* 2004; 43:7902–7915. [PubMed: 15578824]
25. Yu F, Cangelosi VM, Zastrow ML, Tegoni M, Plegaria JS, Tebo AG, Mocny CS, Ruckthong L, Qayyum H, Pecoraro VL. *Chem. Rev.* 2014; 114:3495–3578. [PubMed: 24661096]
26. Touw DS, Nordman CE, Stuckey JA, Pecoraro VL. *Proc. Natl. Acad. Sci. U. S. A.* 2007; 104:11969–11974. [PubMed: 17609383]
27. Chakraborty S, Touw DS, Peacock AFA, Stuckey J, Pecoraro VL. *J. Am. Chem. Soc.* 2010; 132:13240. [PubMed: 20825181]
28. Chakraborty S, Iranzo O, Zuiderweg ERP, Pecoraro VL. *J. Am. Chem. Soc.* 2012; 134:6191–6203. [PubMed: 22394049]
29. Iranzo O, Chakraborty S, Hemmingsen L, Pecoraro VL. *J. Am. Chem. Soc.* 2011; 133:239–251. [PubMed: 21162521]
30. Peacock AFA, Stuckey JA, Pecoraro VL. *Angew. Chem. Int. Ed.* 2009; 48:7371–7374.
31. Ruckthong L, Zastrow ML, Stuckey JA, Pecoraro VL. *J. Am. Chem. Soc.* 2016; 138:11979–11988. [PubMed: 27532255]
32. Zastrow ML, Peacock AFA, Stuckey JA, Pecoraro VL. *Nat. Chem.* 2011; 4:118–123. [PubMed: 22270627]
33. DeLano, WL. *The PyMOL Molecular Graphics System.* Palo Alto, California, USA: DeLano Scientific; 2005. <http://www.pymol.org>
34. Matzapetakis M, Farrer BT, Weng T-C, Hemmingsen L, Penner-Hahn JE, Pecoraro VL. *J. Am. Chem. Soc.* 2002; 124:8042–8054. [PubMed: 12095348]
35. Hemmingsen L, Stachura M, Thulstrup PW, Christensen NJ, Johnston K. *Hyperfine Interact.* 2010; 197:255–267.
36. Hemmingsen L, Sas KN, Danielsen E. *Chem. Rev.* 2004; 104:4027–4062. [PubMed: 15352785]
37. Peacock AFA, Hemmingsen L, Pecoraro VL. *Proc. Natl. Acad. Sci. U. S. A.* 2008; 105:16566–16571. [PubMed: 18940928]
38. Lee K-H, Cabello C, Hemmingsen L, Marsh ENG, Pecoraro VL. *Angew. Chem. Int. Ed.* 2006; 45:2864–2868.
39. Wilkins, RG. *Kinetics and Mechanism of Reactions of Transition Metal Complexes.* 2nd. Weinheim, FRG: Wiley-VCH Verlag GmbH & Co. KGaA; 1991.
40. Ducommun Y, Laurency G, Merbach AE. *Inorg. Chem.* 1988; 27:1148–1152.
41. Danielsen E, Jorgensen L, Sestoft P. *Hyperfine Interact.* 2002; 142:607–626.
42. Shukla D, Hernández CX, Weber JK, Pande VS. *Acc. Chem. Res.* 2015; 48:414–422. [PubMed: 25625937]
43. Jacewicz A, Trzemecka A, Guja KE, Plochocka D, Yakubovskaya E, Bebenek A, Garcia-Diaz M. *PLoS One.* 2013; 8:e76700. [PubMed: 24116139]
44. Saen-Oon S, Ghanem M, Schramm VL, Schwartz SD. *Biophys. J.* 2008; 94:4078–4088. [PubMed: 18234834]
45. Zacate MO, Favrot A, Collins GS. *Phys. Rev. Lett.* 2004; 92:225901. [PubMed: 15245240]

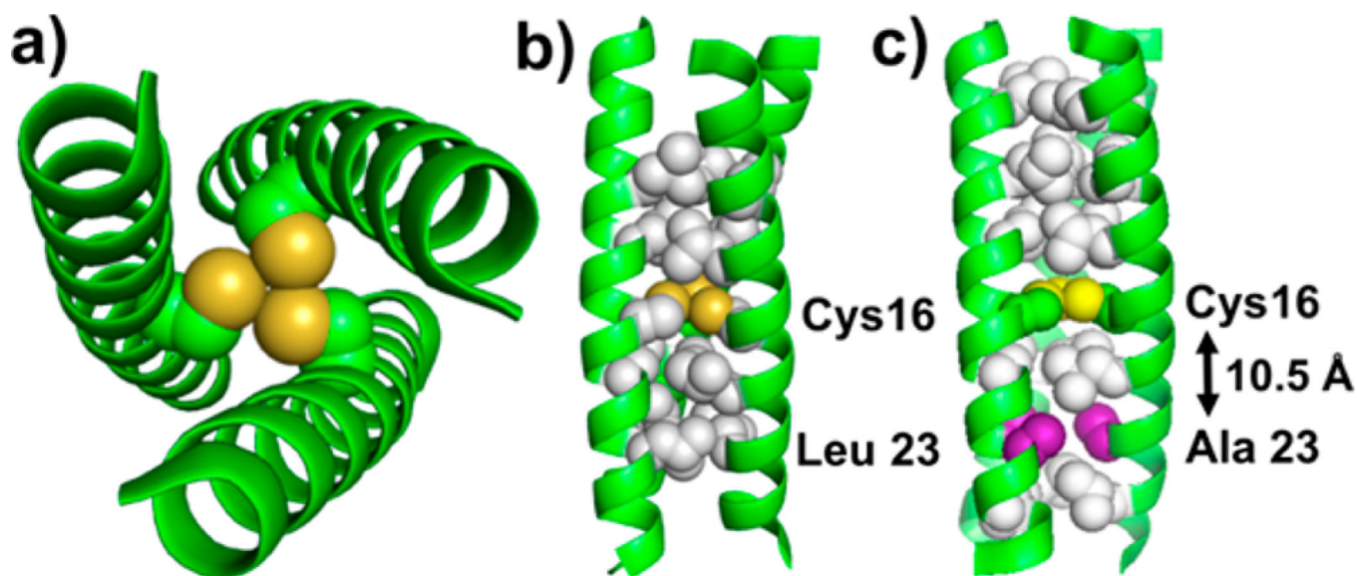


Figure 1. Models of 3SCC used in this study. (a) N \rightarrow C terminus view of **TRIL16C** showing the three Cys residues at the metal site. (b) **TRIL16C** oriented perpendicular to the helical axis. Cys16 and the closest Leu layers are shown explicitly. (c) **TRIL16CL23A** with indication of the Leu23Ala substitution (purple). Protein backbone is shown as green cartoon, thiol groups of Cys as yellow spheres, and Leu layers as white spheres. The model was generated using a 3SCC (Coil Ser) PDB ID 3H5G³⁰ and PyMol.³³

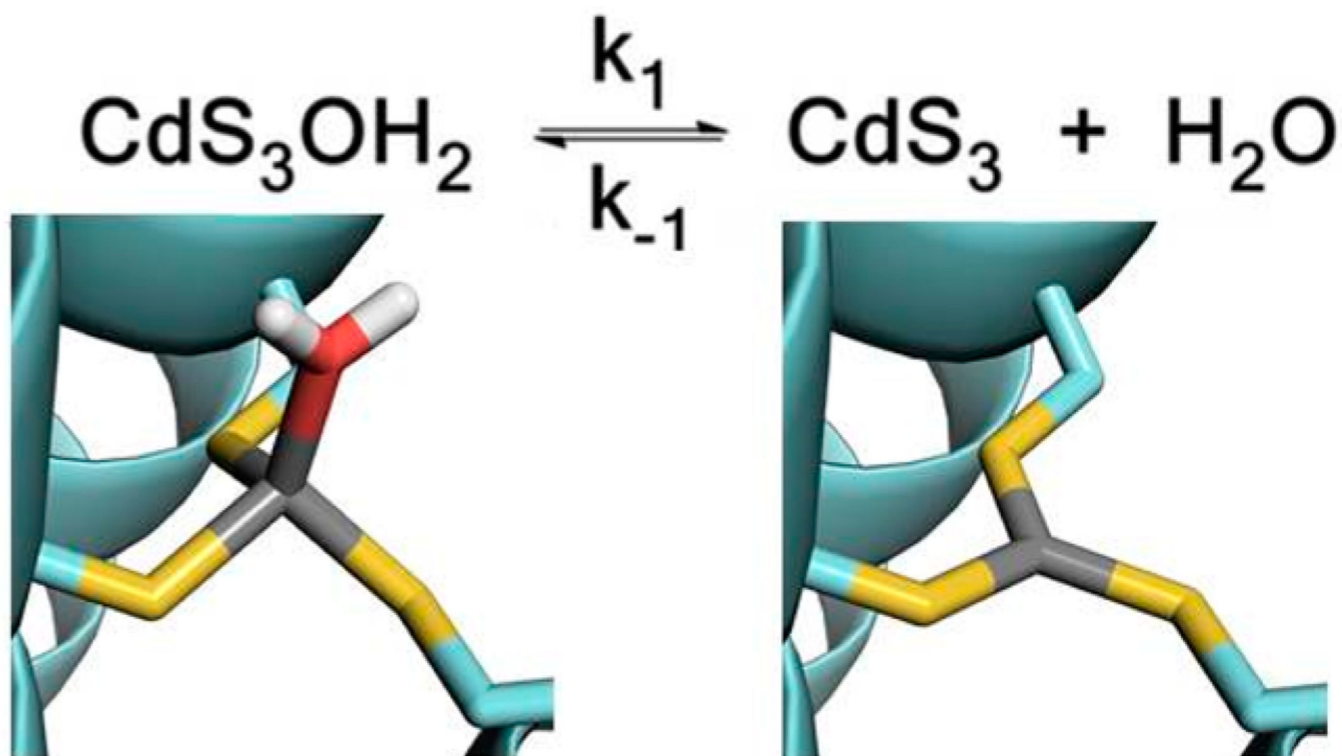


Figure 2. Schematic of the water exchange reaction. The peptide backbone is shown in pale blue, Cys in pale blue and yellow sticks, Cd²⁺ in gray, and water in red and white. The Cd²⁺ binding sites were modeled based on the structure of CSL9C (PDB ID 3LJM).²⁷

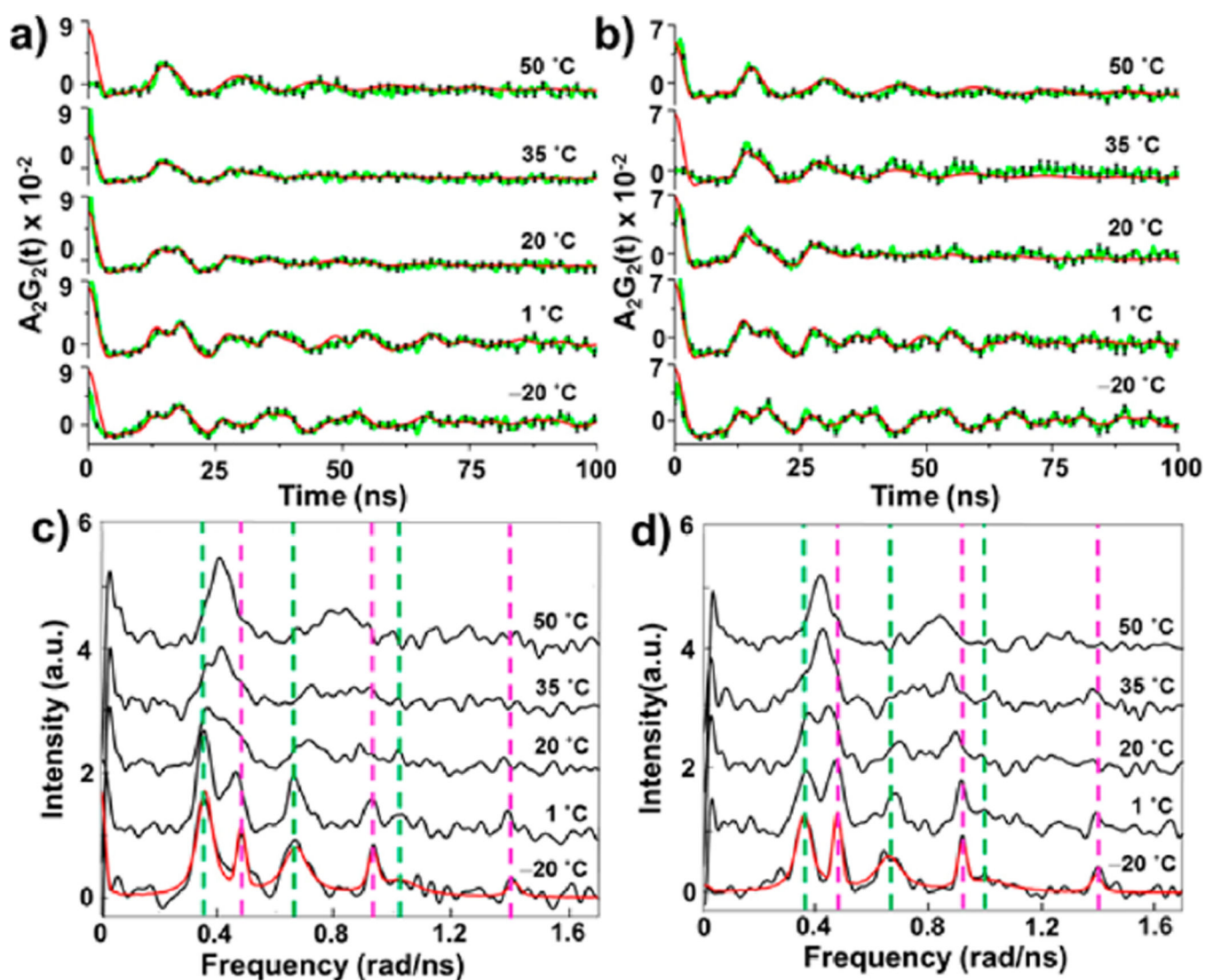


Figure 3. ^{111}mCd PAC spectra at different temperatures for **TRIL16C** (a) and **TRIL16CL23A** (b). Experimental data are shown as green lines connecting data points, fits as red lines, and error bars as black lines. Fourier transformed ^{111}mCd PAC spectra for **TRIL16C** (c) and **TRIL16CL23A** (d) at different temperatures. Experimental data are shown as black lines. Fits to the data at -20 °C for both peptides are shown as red lines. Each coordination geometry gives rise to one NQI, appearing as three peaks in the spectra. Representative signals from the CdS_3O and CdS_3 species are indicated with green and magenta vertical lines, respectively.

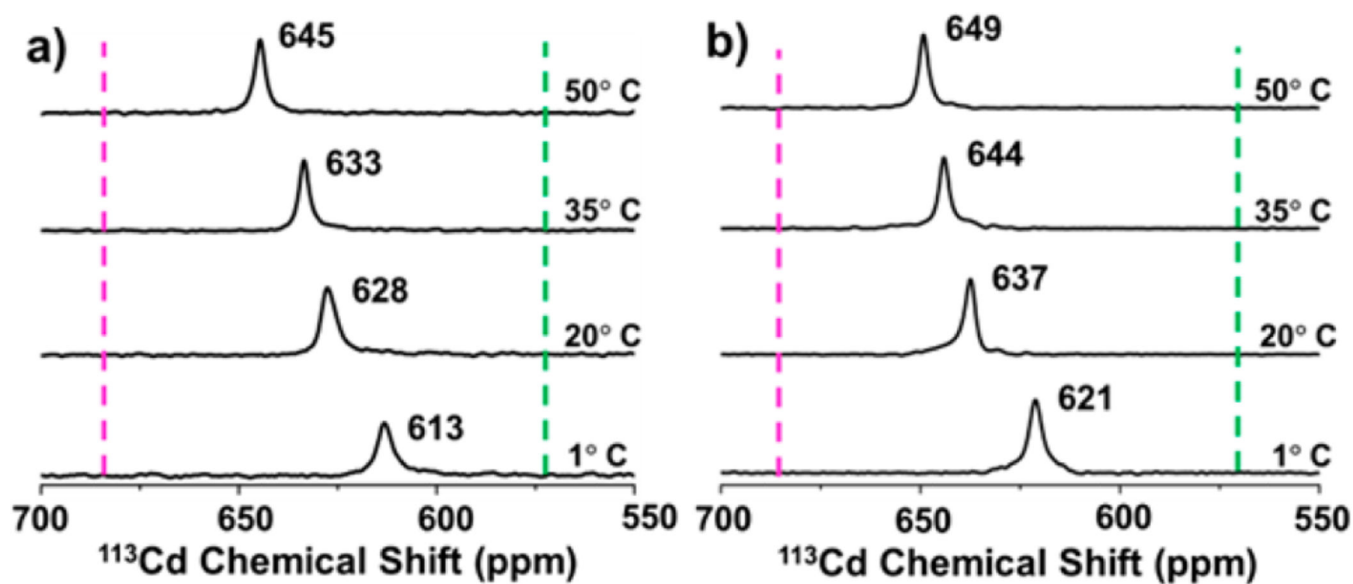


Figure 4. ^{113}Cd NMR spectra of **TRIL16C** (a) and **TRIL16CL23A** (b) with indication of representative chemical shifts observed for pure CdS_3O (green vertical lines) and CdS_3 (magenta vertical lines) species.⁴¹

Table 1Lifetimes of the CdS₃O (τ_1) and CdS₃ (τ_{-1}) Species Derived from the ¹¹¹mCd PAC Data^a

| <i>t</i> [°C] | TRIL16C | | TRIL16CL23A | |
|---------------|---------------|------------------|---------------|------------------|
| | τ_1 [ns] | τ_{-1} [ns] | τ_1 [ns] | τ_{-1} [ns] |
| 1 | 55 | 40 | 44 | 45 |
| 20 | 30 | 23 | 25 | 29 |
| 35 | 17 | 16 | 13 | 15 |
| 50 | 12 | 11 | 6 | 7 |

^aThe statistical standard deviation of the lifetimes is ~1 ns, but does not include errors due to assumptions in the model (see the SI).

Author Manuscript

Author Manuscript

Author Manuscript

Author Manuscript